Available online at www.sciencedirect.com
ScienceDirect
Progress in Natural Science 19 (2009) 471–478
Progress in Natural Science
www.elsevier.com/locate/pnsc

User-controllable mesh segmentation using shape harmonic signature

Yongwei Miao [a,b], Jieqing Feng [a,*], Jinrong Wang [a,c], Xiaogang Jin [a]

[a] State Key Laboratory of CAD & CG, Zhejiang University, Hangzhou 310027, China
[b] College of Science, Zhejiang University of Technology, Hangzhou 310032, China
[c] Information Science & Engineering School, Hangzhou Normal University, Hangzhou 310036, China

Received 14 April 2008; received in revised form 14 June 2008; accepted 16 June 2008

Abstract

Due to different shape modeling applications, partitioning a given complex 3D mesh model into some patches or meaningful subparts is one of the fundamental problems in digital geometry processing. By using the high-dimensional mean-shift clustering scheme in shape signature space, a new method is proposed which can generate user-specified segmentation results automatically for different applications. The shape signature is composed of mesh geometric attributes and its spectral harmonics. The latter one can reflect mesh frequency spectrum information. The low frequency components are essential for semantics-oriented segmentation, while the high frequency components are important for purely geometry-oriented segmentation. The effects of the proposed method are demonstrated by several examples.

Keywords: Mesh segmentation; Manifold harmonic analysis; Shape harmonic signature; Mean-shift clustering

1. Introduction

The problem of partitioning a polygonal mesh into patches or meaningful subparts has been studied in digital geometry processing for different applications, such as texture mapping and texture atlas generation [1,2], surface remeshing and mesh simplification [3,4], skeleton extraction [5], shape morphing and metamorphosis [6,7], shape recognition and shape retrieval [8], and shape modeling [9].

Due to different applications, the mesh segmentation methods can be classified into part-type ones (in a more semantics-oriented manner) and patch-type ones (in a purely geometric sense). The former aims at partitioning the mesh into distinct semantic or meaningful parts according to its shape features, e.g. a head and the legs of a horse, without topological restriction for the segmented parts. The latter one aims at partitioning the underlying mesh into topological disk-like patches based on the mesh geometry features, such as planarity, convexity and curvature.

According to the spectral analysis of a 3D model [10,11], the high frequency signals contribute to the geometric details, while the low frequency signals account for the overall or global shape. In general, when the 3D spectral information is considered, the mesh segmentation based on low frequency information corresponds to the semantics-oriented one, while the mesh segmentation based on high frequency information corresponds to the geometry-oriented one. The mesh segmentation method considered in this paper focuses on both the aspects, and it is an user-controllable scheme.

The proposed method is based on a high-dimensional adaptive mean-shift clustering scheme in shape signature space, where the shape signature is composed of mesh spectral harmonics and its geometric attributes. Unlike the traditional parametric segmentation methods, the proposed one is a non-parametric mean-shift clustering

* Corresponding author. Tel.: +86 571 88206681x506; fax: +86 571 88206680.
E-mail address: jqfeng@cad.zju.edu.cn (J. Feng).

1002-0071/$ - see front matter © 2008 National Natural Science Foundation of China and Chinese Academy of Sciences. Published by Elsevier Limited and Science in China Press. All rights reserved.
doi:10.1016/j.pnsc.2008.06.024

scheme, which need not specify the cluster number in advance.

The contributions of the proposed method are summarized as follows:

(1) Based on the manifold harmonic analysis, a new definition of the shape harmonic signature is proposed, which can be used for the subsequent clustering analysis.
(2) The traditional mean-shift analysis is extended to the high-dimensional and adaptive cases.
(3) By choosing different signatures in the shape signature space, the method can be tailored to the specified segmentation purposes.

The paper is organized as follows: The related works are briefly reviewed in Section 2. The multi-dimensional shape signature is defined in Section 3, which is based on both the frequency spectrum information and the geometric information. The adaptive mean-shift analysis is adopted for robust shape signatures clustering, which is described in Section 4. Some examples of user-controlled mesh segmentations are given in Section 5. Finally, conclusions are drawn, and the future researches are discussed in Section 6.

2. Related work

Various model segmentation methods have been proposed in digital geometry processing, such as the clustering ones, the region-growing ones, the watershed ones, the geometric snake ones, and the spectral analysis ones. Readers interested in more details can refer to the thorough survey by Shamir [12].

One automatic approach is to partition a polygonal mesh into a set of face clusters through the greedy face clustering method, where each face cluster can be approximated by a fitting plane [13]. By adopting other fitting primitives, Attene et al. [14] segmented a mesh into face clusters hierarchically where each face cluster can be best fit by not only plane, but also sphere or cylinder. Katz and Tal [5] hierarchically decomposed a mesh by using the fuzzy clustering method based on geodesic and angular distances of the dual graph of the given mesh. Yamauchi et al. [15] proposed a mesh normal mean-shift clustering method and achieved a feature-sensitive mesh segmentation. Reniers and Telea [16] presented a hierarchical and level-of-detail shape segmentation method that can segment a 3D model into meaningful component sets associated with critical points on its curve skeleton. Inspired by Lloyd's max quantization method, Shlafman et al. [7] proposed a k-means clustering method to decompose a mesh into some meaningful parts in which the clustering metric is determined by the dihedral angle and the "physical" distance between the faces. According to the hierarchical mesh structures generated by the feature-sensitive isotropic remeshing method, Lai et al. [17] proposed a k-means clustering-based top–down hierarchical segmentation algorithm. Recently, Miao et al. [18] presented a k-means point-sampled geometry clustering method, which is based on the Euclidean distance variation between sample points and angular difference variation between differential directions on the surface.

The region-growing-based mesh segmentation method is closely related with the clustering ones. The generated charts grow so as to align their boundaries with the high curvature features of the mesh [19]. To generate charts which can be flattened efficiently in mesh parameterization, Yamauchi et al. [20] proposed an integrated Gaussian curvature-based segmentation method that measures the developability of a chart. It can evenly distribute Gaussian curvature over the charts and automatically ensure disc-like topology of each chart.

Inspired by image processing research, the watershed-based method can partition a mesh into several subparts. The earlier watershed-based method proposed by Magan and Whitaker [21] tends to align the boundaries along with the high curvature regions and neglects the concavity regions. Page et al. [22] proposed a fast marching watershed algorithm where the height map is adopted to avoid climbing up negative principal curvature hills. As an extension of the active snake model, Lee et al. [23] adopted the geometric snake as an interactive tool for the feature detection and the mesh segmentation, in which an initial segmentation curve slithers from a user-specified position to a nearby feature curve through minimizing an energy functional.

Recently, several frequency-domain-based techniques have been proposed. According to the spectral analysis of the combinatorial graph Laplacian, Gotsman [24] proposed a geometric space partitioning technique. Due to a pose-invariant representation of a mesh based on the multi-dimensional scaling analysis, Katz et al. [25] extracted the prominent feature points near the extremities of an articulated shape and obtained the key components of a mesh, which can generate an efficient segmentation. Moreover, by using the spectral analysis-based k-means clustering on the mesh affinity matrix, Liu et al. [26] developed a mesh segmentation along the mesh concave regions. Based on 2D spectral embedding and 2D contour analysis from the planar embedding using graph Laplacian and geometric operators, Liu et al. [27] also presented a nearly automatic mesh part-type segmentation algorithm by iteratively bisecting a sub-mesh.

The above-mentioned segmentation methods are parametric ones, that is, users should provide the clustering number in advance, and each element (vertices or sample points) should be assigned to one of them initially. It is not always a trivial work to specify a clustering number. However, the proposed segmentation scheme is a non-parametric mean-shift iterative one. Users need not specify the clustering number in advance, which can be automatically altered with the algorithm processing. Moreover, the proposed approach can take the mesh spectral harmonics and its geometric attributes into account simultaneously.

Thus, users can control the segmentation by adjusting their corresponding weights.

3. Shape harmonic signature

Based on the combinatorial graph Laplacian operators, Taubin [11] first introduced the spectral analysis as a digital geometry signal processing tool. Due to the sole dependence on the vertex connections, the graph Laplacian operator was later improved as the discrete Laplacian operator [28,29], which replaces the uniform weights with the more elaborate cotangent weights. Because the coefficients of the discrete Laplacian operator are non-symmetric, the operator seemingly loses an important property of its continuous counterparts, i.e., the orthogonality of eigenvectors. In our framework, the multiple orthogonal eigenfunctions are computed and a different shape signature is defined.

In order to conduct the classical Fourier spectral analysis on the 3D geometry, Pauly et al. [10] parameterized a 3D discrete point cloud on a parametric plane. Due to the robustness of spherical parameterization, Zhou et al. [30] defined a 3D sphere as the base domain and adopted the spherical harmonics for the geometry processing. Note that these methods generally require a parameterization and subsequent resampling procedures. However, it is difficult to perform the two preprocessing procedures robustly and efficiently in general. To avoid them, it is necessary to directly compute its frequency spectrum for a mesh of arbitrary topology. The manifold analysis and exterior calculus, similar to the analysis framework as Vallet and Levy [31], is an alternative tool to facilitate the goal.

The classical Laplacian definition can be generalized to a manifold version S with a metric g, namely the Laplace–Beltrami operator [32]:

$$\triangle_S = div \cdot grad = \sum_i \frac{1}{\sqrt{|g|}} \frac{\partial}{\partial x_i} \sqrt{|g|} \frac{\partial}{\partial x_i}$$

where $|g|$ denotes the determinant of metric g. The manifold harmonics are the solution of the following manifold harmonic equation:

$$-\triangle_S h = \lambda h$$

Using "hat" functions $\Phi^j (j = 1, 2, \ldots, n)$ related to each vertex (that is piecewise-linear function on the triangles and satisfies $\Phi^j(v_j) = 1$ and $\Phi^j(v_k) = 0$ if $k \neq j$) as test and basis functions, the equation can be rewritten as the projection form:

$$-\langle \triangle_S h, \Phi^j \rangle = \lambda \langle h, \Phi^j \rangle, \quad \text{for } \forall j$$

Solving the above projection equation by the finite element technique is equivalent to finding out the function in the form of $h = \sum_{i=1}^{n} h_i \Phi^i$, which satisfies the following linear system:

$$-\sum_{i=1}^{n} h_i \langle \triangle_S \Phi^i, \Phi^j \rangle = \lambda \sum_{i=1}^{n} h_i \langle \Phi^i, \Phi^j \rangle, \quad \text{for} \quad \forall j$$

By computing the stiffness matrix $\boldsymbol{Q} = (Q_{ij})$ where $Q_{ij} = \langle \triangle_S \Phi^i, \Phi^j \rangle$ and mass matrix $\boldsymbol{B} = (B_{ij})$ where $B_{ij} = \langle \Phi^i, \Phi^j \rangle$, the matrix form of the above equation is

$$-\boldsymbol{Q}h = \lambda \boldsymbol{B}h$$

or

$$-\boldsymbol{B}^{-1}\boldsymbol{Q}h = \lambda h$$

which can be solved by utilizing the spectral shift technique [31].

According to the spectral analysis, low frequency signals account for the global geometric shape, while high frequency signals contribute to the geometric details (see Fig. 1). Thus, the low frequency components are essential for the semantics-oriented segmentation. On the other hand, to segment a model along the geometric features, such as folds and wrinkles, the high frequency components are important for the purely geometry-oriented segmentation.

These frequency signals can be intrinsically characterized by the manifold harmonics (see Figs. 1 and 2). Fur-

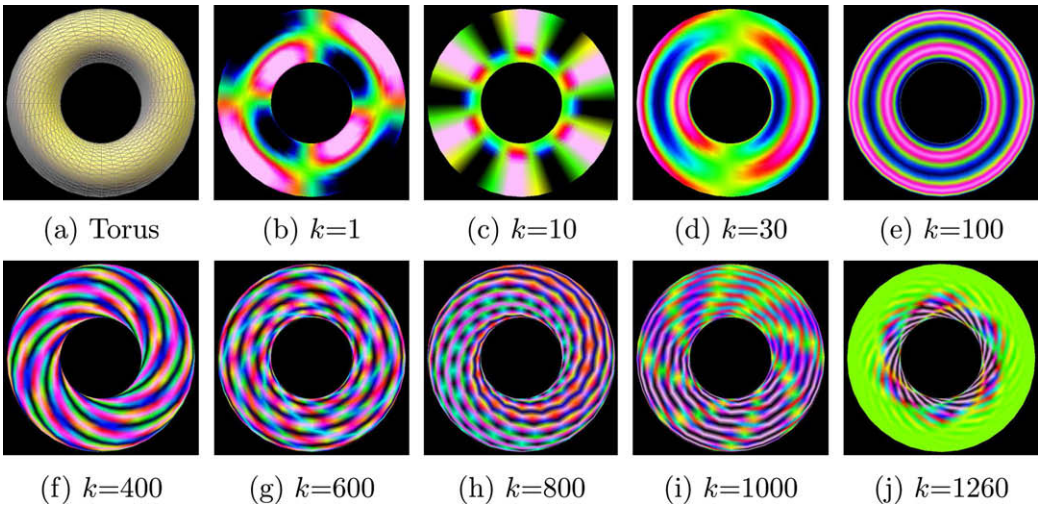

Fig. 1. Selected shape harmonics of the Torus model.

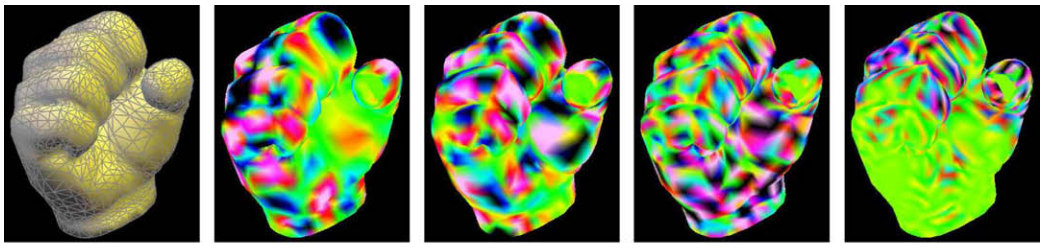

(a) Hand (b) k=50 (c) k=100 (d) k=300 (e) k=800

Fig. 2. Selected shape harmonics of the Hand model.

thermore, the evaluated manifold harmonics can be regarded as the discrete values attached to each vertex and continuous piecewise-linear functions could be reconstructed on the whole mesh. These shape harmonics can reflect the intrinsic geometric attributes associated on the vertices. Any subset of those attributes can be chosen and designed to characterize the signature space. In detail, for each vertex v, its harmonic signature information $\boldsymbol{H}(v)$ can be defined in a joint space of both geometry and manifold harmonic attributes. It comprises four different parts. The first two parts are the spectral information, i.e., low frequency and high frequency information. The other two parts are its spatial information, including position v_x, v_y, v_z, and normal n_x, n_y, n_z. The low frequency information contributes to overall shape and is defined as

$$\frac{1}{\sqrt{\lambda_1}}h^1(v),\ \frac{1}{\sqrt{\lambda_2}}h^2(v),\ \frac{1}{\sqrt{\lambda_3}}h^3(v),\ \ldots$$

The high frequency information is related with geometric details and is defined as

$$\frac{1}{\sqrt{\lambda_n}}h^n(v),\ \frac{1}{\sqrt{\lambda_{n-1}}}h^{n-1}(v),\ \frac{1}{\sqrt{\lambda_{n-2}}}h^{n-2}(v),\ \ldots$$

In the signature space, the user can interactively specify signatures for the different segmentation objectives. For example, to segment a mesh into meaningful parts, it should include the low frequency signatures

$$I = \left(\frac{1}{\sqrt{\lambda_1}}h^1(v),\ \frac{1}{\sqrt{\lambda_2}}h^2(v),\ \ldots,\ \frac{1}{\sqrt{\lambda_k}}h^k(v)\right)$$

However, to segment a mesh into patches along high curvature features, it should include the high frequency signatures

$$II = \left(\frac{1}{\sqrt{\lambda_n}}h^n(v),\ \frac{1}{\sqrt{\lambda_{n-1}}}h^{n-1}(v),\ \ldots,\ \frac{1}{\sqrt{\lambda_{n-l}}}h^{n-l}(v)\right)$$

If the segmentation is based on spatial information, the signature should also comprise the following spatial components:

$$III = (v_x, v_y, v_z)$$

and

$$IV = (n_x, n_y, n_z)$$

Thus, according to different segmentation applications, the final signatures for a vertex v can be chosen as the linear combination of the above four signatures.

4. Adaptive mean-shift clustering in harmonic signature feature space

Based on the analysis of the multi-modal shape signature space defined in both frequency and spatial domain spaces, the mean-shift method [33,34] will be a powerful non-parametric feature space clustering technique for high-dimensional scattered data. The shape signature feature space itself can be regarded as an empirical probability density function. The traditional mean-shift scheme is an ascending search technique for the local maxima along the increasing direction of the density function gradient [35]. Applying this scheme to a set of given discrete data points will create clusters around the maxima modes, which correspond to the dense regions in the feature space. Unlike many other parametric clustering techniques which should specify the number of modes or clusters as a prerequisite, this scheme can determine it automatically by the mean-shift procedure itself.

In the traditional fixed bandwidth mean-shift clustering scheme, the neighbor points within a fixed radius region will depend heavily on the distribution of high-dimensional data points in the feature space, e.g., it may be sparse or dense in the feature space. The sampling irregularity may lead to incorrect clustering results [36]. In our adaptive mean-shift clustering, for each data point p in the d-dimensional feature space R^d, the key step is to determine the appropriate size of the neighborhood $N(p)$ and the associated adaptive bandwidth value $h(p)$ as follows:

$$h(p) = max_{q\in N(p)}(dist(p,q))$$

For the sake of simplicity, we adopt the K-nearest neighboring method to determine the neighbors of data points.

First, the procedure computes the weighted average of the data points which falls inside this neighborhood window, and then iteratively moves the window to the mean point. In general, the weighted mean of a feature data point p in the joint feature space can be defined by a monotonically decreasing symmetric profile kernel $g(x)$ with a radius $h(p)$ in the feature space, such as the Gaussian kernel or the Epanechnikov kernel [33,34]. The mean shift local mode

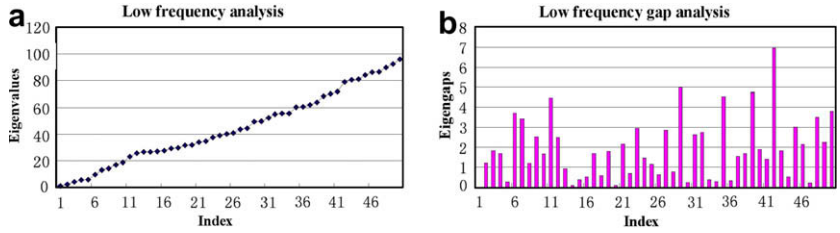

Fig. 3. Low frequency analysis for the Eight model. (a) Frequency analysis for the first 50 low frequency components and (b) their corresponding eigengaps.

$M_h(p)$ in the feature space can be generated by the following iteration procedures:

$$M_h^v(p) := \frac{\sum_{q\in N(p)} q/h^{d+2} g\left(\|dist(p,q)/h\|^2\right)}{\sum_{q\in N(p)} 1/h^{d+2} g\left(\|dist(p,q)/h\|^2\right)} - M_h(p)$$

$$M_h(p) := M_h(p) + M_h^v(p)$$

where $M_h(p)$ is also called the mean-shift point whose initial value can coincide with p, and $M_h^v(p)$ is the mean-shift vector associated with the adaptive bandwidth.

For the data points in a high-dimensional feature space, the bottleneck and time-consuming step of the mean-shift clustering is to search the closest neighbors. Due to its computational complexity, the traditional approach based on the Kd-tree is inefficient. Similar to the locally sensitive hashing search method described in [36,37], the approximately nearest neighbor search algorithm is adopted for determining the k-nearest neighbors of each data point in the feature space.

According to the user-specified vertex shape signatures in the feature space, our adaptive mean-shift clustering algorithm can be performed through the following steps according to different mesh segmentation objectives:

(1) For each vertex v, its harmonic signature $\boldsymbol{H}(v)$ is computed.
(2) A multi-dimensional mean-shift iterative procedure is then applied to its local modes computation.
(3) For each local maximal mode, a cluster is generated by assigning each vertex to its nearest local mode; the distance between the signatures can be computed as the weighted sum of each signature component, that is

$$dist(\boldsymbol{H}(v_i), \boldsymbol{H}(v_j)) = \omega_1\|I(v_i) - I(v_j)\| + \omega_2\|II(v_i) - II(v_j)\| + \omega_3\|III(v_i) - III(v_j)\| + \omega_4\|IV(v_i) - IV(v_j)\|$$

Each cluster will be assigned with an average signature and its vertex number.
(4) According to the number of the vertex, these clusters are sorted descendingly.
(5) Those clusters whose size is below a user-specified threshold are pruned, and the pruned vertices are reassigned to their nearest cluster.

5. Experimental results and discussion

All the algorithms presented in this paper are implemented and tested on a PC with a Pentium 4 2.0 GHz

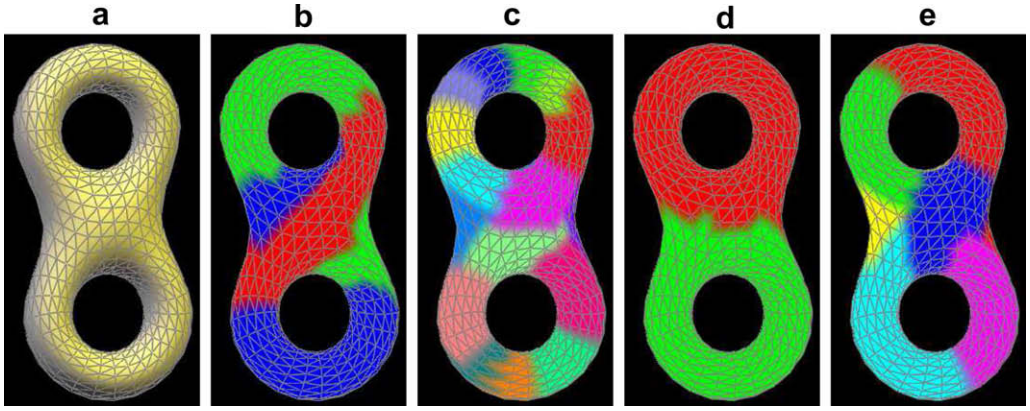

Fig. 4. Partitioning the Eight model by manifold harmonic signatures and position information. (a) Original model; (b and c) semantics-oriented segmentation by low frequency manifold harmonic signatures, in which the first 3 and 10 low frequency signatures are selected, respectively; (d and e) semantics-oriented segmentation by the combination of manifold harmonic signatures and position information, in which the weights of the first 10 low frequency signatures and position are 0.3, 0.7, and 0.7, 0.3, respectively.

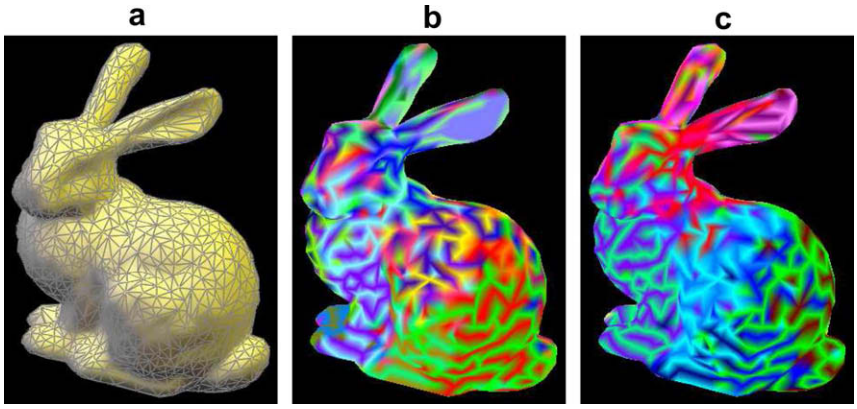

Fig. 5. Partitioning by manifold frequency and surfel information. (a) Original Stanford bunny model; (b and c) geometry-oriented segmentation by the combination of manifold harmonic signatures and surfel information, in which weights of the last 10 high frequency signatures, position and normal information are 0.3, 0.2, 0.5 and 0.6, 0.3, 0.1, respectively.

CPU, 512M memory and Windows XP. In our algorithm, the vertex harmonic signature $\boldsymbol{H}(v)$ is an important determinant in the final segmentation. As mentioned in Section 3, due to different segmentation purposes, users can select different signatures or their combination for each vertex, including low frequency harmonic, high frequency harmonic and spatial information.

Segmentation only by manifold harmonic frequency. According to matrix perturbation theory [38,39], there exist some intrinsic connections between the gaps of eigenvalues and the cohesiveness of the clusters. For the sake of part-type segmentation by low frequency signals, we can choose the first several sequential harmonic signatures until the first large eigengap is encountered, which could generate the semantics-oriented segmentation (see Fig. 4b and c). On the contrary, for patch-type segmentation by high frequency signals, the last several sequential harmonic signatures are selected until the last large eigengap is encountered to generate the purely geometric sense segmentation (see Fig. 5). For the Eight model, according to the frequency analysis (see Fig. 3), the first 3 or 10 low frequency signatures can be selected for semantics-oriented segmentation (see Fig. 4b and c). In general, if the user takes more shape harmonic signatures into account, it will generate more subparts.

Fig. 6 shows some semantics-oriented segmentation results for different models. All the experimental results in this figure are generated by the mean-shift clustering of

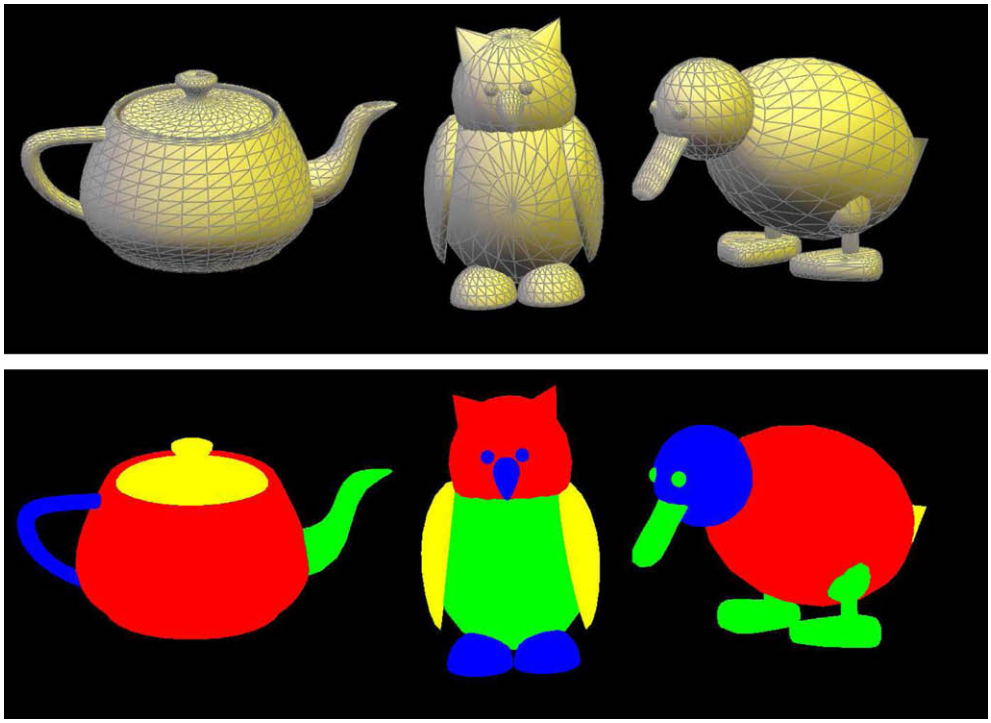

Fig. 6. Semantics-oriented segmentation by low frequency manifold harmonic signatures. Upper row: different original models; Bottom row: semantics-oriented segmentation results by the low frequency harmonic signatures, in which the first 3, 10, and 12 low frequency signatures are selected for teapot, penguin, and duck, respectively.

the first several low frequency signatures. For example, the semantics-oriented segmentation for teapot, penguin, and duck is generated by using the first 3, 10, and 12 low frequency signatures, respectively.

Partitioning by manifold harmonic frequency and position information. The frequency spectrum information and its geometric attributes can also be combined together as the segmentation signature. It corresponds to different applications of mesh segmentation. For the Eight model, the first 10 low frequency signatures and position information are selected to perform semantics-oriented segmentation. In Fig. 4d, the weights of the frequency signatures and position information are 0.3 and 0.7, respectively, while in Fig. 4e they are 0.7 and 0.3, respectively.

Partitioning by manifold harmonic frequency and surfel information. Finally, partitioning the underlying model according to its frequency signatures and its sample surfel (vertex position and normal information) will lead to a user-specified segmentation. For the Stanford bunny model, Fig. 5b shows the segmentation result that is obtained by choosing the last 10 high frequency signatures and surfel information, in which weights of the last 10 high frequency signatures, position and normal information are 0.3, 0.2, and 0.5, respectively, while Fig. 5c shows the segmentation result that is obtained by choosing similar shape signatures, and the weights are 0.6, 0.3, and 0.1, respectively. Our experiments show that the large weight of the high frequency signatures emphasizes the geometric details of the underlying model, such as folds and wrinkles, while the large weight of the position or normal information will emphasize the compactness or planarity of the underlying model.

6. Conclusions and future work

A new mesh segmentation approach is proposed, which is based on an adaptive mean-shift clustering scheme on the shape harmonic signature and geometry information space. Our signature feature space is defined as a multi-dimensional one associated with the surface spectral harmonics and its geometric attributes. According to the traditional spectral analysis, low frequency signals account for the overall geometric shape, while high frequency signals contribute to the geometric details. Thus, the low frequency component is essential for the semantics-oriented segmentation. On the contrary, to segment a model along the folds and wrinkles, the high frequency component is important for the purely geometric segmentation. According to the user pre-defined shape signatures, it is possible to partition the given mesh according to the user's different partition objectives.

However, like the common spectral clustering algorithms for mesh segmentation [25,26], our current approach can generate natural segmentation results only for mesh models on which the visually salient segmentation boundaries are mostly around concave regions, otherwise a post-processing step should be adopted to smoothen the coarse boundaries by finding a minimum cut [5] or by using geometric snakes [23]. Furthermore, the bottleneck of our segmentation framework is the low efficiency of computing harmonic frequency spectrum for large-scale 3D models. In order to overcome this limitation, multi-thread parallel scheme and TAUCS solvers [40] can be adopted to calculate the eigen systems of a large harmonic problem, and GPU techniques can also be employed to accelerate our shape analysis system.

In the future, more shape analysis and editing operations based on harmonic frequency spectral analysis will be investigated, for example, shape remeshing, digital watermark, detail transfer, and deformation transfer.

Acknowledgements

The work was jointly supported by National Natural Science Foundation of China (Grant Nos. 60743002 and 60736019), the China Postdoctoral Science Foundation (Grant No. 20070421184), the Doctoral Program of Higher Education (Specialized Research Fund Grant No. 20050335069), and the Natural Science Foundation of Zhejiang Province (Grant Nos. Y107311 and R106449).

References

[1] Zhang E, Mischaikow K, Turk G. Feature based surface parameterization and texture mapping. ACM Trans Graph 2005;24(1):1–27.
[2] Zhou K, Snyder J, Guo B, et al. Iso-charts: stretch-driven mesh parameterization using spectral analysis. In: Proceedings of the Eurographics symposium on geometry processing, July 8–10, France: Nice; 2004. p. 47–56.
[3] Cohen-Steiner D, Alliez P, Desbrun M. Variational shape approximation. ACM Trans Graph 2004;23(3):905–14.
[4] Dong S, Bremer P-T, Garland M, et al. Spectral surface quadrangulation. ACM Trans Graph 2006;25(3):1057–66.
[5] Katz S, Tal A. Hierachical mesh decomposition using fuzzy clustering and cuts. ACM Trans Graph 2003;22(3):954–61.
[6] Gregory A, State A, Lin M, et al. Interactive surface decomposition for polyhedral morphing. Visual Comput 1999;15(9):453–70.
[7] Shlafman S, Tal A, Katz S. Metamorphosis of polyhedral surfaces using decomposition. Comput Graph Forum 2002;21(3):219–28.
[8] Zuckerberger E, Tal A, Shlafman S. Polyhedral surface decomposition with applications. Comput Graph 2002;26(5):733–43.
[9] Funkhouser T, Kazhdan M, Shilane P, et al. Modeling by example. ACM Trans Graph 2004;23(3):652–63.
[10] Pauly M, Gross M. Spectral processing of point-sampled geometry. In: Proceedings of ACM SIGGRAPH, August 12–17, Los Angeles, California, USA; 2001. p. 379–86.
[11] Taubin G. A signal processing approach to fair surface design. In: Proceedings of ACM SIGGRAPH, August 6–11, Los Angeles, California, USA; 1995. p. 351–8.
[12] Shamir A. Segmentation and shape extraction of 3D boundary meshes. In: Proceedings of eurographics, September 4–8, Vienna, Austria; 2006. p. 137–49.
[13] Garland M, Willmott A, Heckbert P. Hierarchical face clustering on polygonal surfaces. In: Proceedings of ACM symposium on interactive 3D graphics, March 26–29, North Carolina, USA; 2001. p. 49–58.
[14] Attene M, Falcidieno B, Spagnuolo M. Hierarchical segmentation based on fitting primitives. Visual Comput 2006;22(3):181–93.
[15] Yamauchi H, Lee S, Lee Y, et al. Feature sensitive mesh segmentation with mean shift. In: Proceedings of the IEEE international

conference on shape modeling and applications, June 15–17, Cambridge, MA, USA; 2005. p. 238–45.
[16] Reniers D, Telea A. Skeleton-based hierarchical shape segmentation. In: Proceedings of the IEEE international conference on shape modeling and applications, June 13–15, Lyon, France; 2007. p. 179–88.
[17] Lai YK, Zhou QY, Hu SM, et al. Feature sensitive mesh segmentation. In: Proceedings of ACM symposium on solid and physical modeling, June 6–8, Cardiff, Wales, United Kingdom; 2006. p. 17–25.
[18] Miao YW, Feng JQ, Xiao CX, et al. Differentials-based segmentation and parameterization for point-sampled surfaces. J Comput Sci Technol 2007;22(5):749–60.
[19] Levy B, Petitjean S, Ray N, et al. Least squares conformal maps for automatic texture atlas generation. ACM Trans Graph 2002;21(3):362–71.
[20] Yamauchi H, Gumhold S, Zayer R, et al. Mesh segmentation driven by Gaussian curvature. Visual Comput 2005;21(8–10):649–58.
[21] Mangan A, Whitaker R. Partitioning 3d surface meshes using watershed segmentation. IEEE Trans Vis Comput Graph 1999;5(4):309–21.
[22] Page DL, Koschan AF, Abidi MA. Perception-based 3D triangle mesh segmentation using fast marching watersheds. In: Proceedings of computer vision and pattern recognition, June 16–22, Madison, WI, USA; 2003. p. 27–32.
[23] Lee Y, Lee S. Geometric snakes for triangular meshes. Comput Graph Forum 2002;21(3):229–38.
[24] Gotsman C. On graph partitioning, spectral analysis, and digital mesh processing. In: Proceedings of the IEEE international conference on shape modeling and applications, May 12–16, Seoul, Korea; 2003. p. 165–74.
[25] Katz S, Leifman G, Tal A. Mesh segmentation using feature point and core extraction. Visual Comput 2005;21(8–10):649–58.
[26] Liu R, Zhang H. Segmentation of 3D meshes through spectral clustering. In: Proceedings of the computer graphics and applications, 12th pacific conference, October 6–8, Seoul, Korea; 2004. p. 298–05.
[27] Liu R, Zhang H. Mesh segmentation via spectral embedding and contour analysis. Comput Graph Forum 2007;26(3):385–94.
[28] Desbrun M, Meyer M, Schroder P, et al. Implicit fairing of irregular meshes using diffusion and curvature flow. In: Proceedings of ACM SIGGRAPH, August 8–13, Los Angeles, California, USA; 1999. p. 317–24.
[29] Meyer M, Desbrun M, Schroder P, et al. Discrete differential-geometry operators for triangulated 2-manifolds. In: Hege H-C, Polthier K, editors. Visualization and mathematics III. Heidelberg: Springer-Verlag; 2003. p. 35–57.
[30] Zhou K, Bao HJ, Shi JY. 3D surface filtering using spherical harmonics. Comput Aided Des 2004;36(4):363–75.
[31] Vallet B, Levy B. Spectral geometry processing with manifold harmonics. Comput Graph Forum 2008;27(2):251–60.
[32] Do Carmo M. Differential geometry of curves and surfaces. Englewood Cliffs, New Jersey: Prentice-Hall; 1976.
[33] Comaniciu D, Meer P. Mean shift analysis and applications. In: Proceedings of IEEE international conference on computer vision, September 20–25, Kerkyra, Corfu, Greece; 1999. p. 1197–203.
[34] Comaniciu D, Meer P. Mean shift: a robust approach toward feature space analysis. IEEE Trans Pattern Anal Mach Intell 2002;24(5):603–19.
[35] Shamir A, Shapira L, Cohen-Or D. Mesh analysis using geodesic mean-shift. Visual Comput 2006;22(2):99–108.
[36] Georgescu B, Shimshoni I, Meer P. Mean shift based clustering in high dimensional: a texture classification example. In: Proceedings of international conference on computer vision, October 13–16, Nice, France; 2003. p. 456–63.
[37] Indyk P, Motwani R. Approximate nearest neighbors: towards removing the curse of dimensionality. In: Proceedings of ACM symposium on theory of computing, May 23–26, Dallas, Texas, USA; 1998. p. 604–13.
[38] Ng AY, Jordan MI, Weiss Y. On spectral clustering: analysis and an algorithm. In: Advances in neural information processing systems, vol. 14, 2002. p. 857–64.
[39] Stewart GW, Sun J-G. Matrix perturbation theory. New York: Academic Press; 1990.
[40] Toledo S. TAUCS: a library of sparse linear solvers, version 2.2, 2003. Available from: http://www.tau.ac.il/~stoledo/taucs/.